Laser and Particle Beams (2016), *34*, 735–741.

doi:10.1017/S0263034616000690

Target implosion uniformity in heavy-ion fusion

T. KARINO,[1] S. KAWATA,[1] S. KONDO,[1] T. IINUMA,[1] T. KUBO,[1] H. KATO,[1] AND A. I. OGOYSKI[2]

[1]Utsunomiya University, Utsunomiya, Graduate school of engineering, Tochigi 321-8585, Japan
[2]Varna Technical University, Department of Physics, Varna 9010, Bulgaria

(RECEIVED 29 July 2016; ACCEPTED 10 October 2016)

Abstract

In this paper, the robustness of the dynamic instability mitigation mechanism is first examined, and then the instability mitigation phenomenon is demonstrated in a deuterium–tritium (DT) fuel target implosion by wobbling heavy-ion beams (HIBs). The results presented here show that the mechanism of the dynamic instability mitigation is rather robust against changes in the phase, the amplitude and the wavelength of the wobbling perturbation applied. In general instability would emerge from the perturbation of the physical quantity. Normally the perturbation phase is unknown, so that the instability growth rate is discussed. However, if the perturbation phase is known, the instability growth can be controlled by a superposition of perturbations imposed actively: if the perturbation is induced by, for example, a driving beam axis oscillation or wobbling, the perturbation phase could be controlled and the instability growth is mitigated by the superposition of the growing perturbations. In this paper, we realize the superposition of the perturbation by the wobbling HIBs' illumination onto a DT fuel target in heavy-ion inertial fusion (HIF). Our numerical fluid implosion simulations present that the implosion non-uniformity is mitigated successfully by the wobbling HIBs illumination in HIF.

Keywords: Heavy-ion beam; Implosion uniformity; Inertial confinement fusion; Non-uniformity mitigation; Rayleigh–Taylor instability

1. INTRODUCTION

In inertial confinement fusion, non-uniformity implosion leads a degradation of fusion energy output. Implosion non-uniformity is introduced by, for example, the Rayleigh–Taylor instability (RTI), the driver beam illumination non-uniform, fuel target imperfect sphericity, etc.

The RTI dynamic stabilization was proposed many years ago (Wolf, 1970; Troyon & Gruber, 1971) in inertial fusion; the oscillation amplitude of the driving acceleration should be sufficiently large to stabilize RTI (Wolf, 1970; Troyon & Gruber, 1971; Boris, 1977; Betti *et al.*, 1993; Piriz *et al.*, 2010, 2011). In inertial fusion, the fusion fuel compression is essentially important to reduce an input driver energy (Nuckolls *et al.*, 1972; Atzeni & Meyer-ter-Vehn, 2004), and the implosion uniformity is one of critical issues to release the fusion energy stably (Emery *et al.*, 1982; Kawata & Niu, 1984). Instability grows from a perturbation of the physical quantity, and the perturbation phase is unknown in plasmas. Therefore, usually the instability growth rate is focused and examined. On the other hand, in an unstable system there is a well-known feedback control mechanism in which the perturbation amplitude and phase are detected, and the growing perturbation is compensated by the active feedback control. However, in plasmas and fluids it is difficult to measure the instability phase and amplitude, and so the perfect active feedback control cannot be realized.

If we actively impose the perturbation phase by the driving energy source wobbling or oscillation, and so if we know or define the phase of the perturbations imposed actively, the perturbation growth can be controlled in a similar way (Kawata *et al.*, 1993, 2009; Kawata, 2012) as the feedback control mechanism. For example, the two-stream instability growth would be controlled by a time-dependent drift velocity of the driving beam. When the driving beam longitude velocity is oscillating, the two-stream instability perturbation phase changes in time. At each time, the driving beam introduces a new perturbation phase, and the actual instability growth is defined by the superposition of all the growing perturbations by the time-dependent drift velocity. The heavy ion accelerator could provide a beam wobbling about a central axis with a high frequency (Moretti, 1982; Kawata *et al.*, 2013). The wobbling heavy-ion beams (HIBs) also define the perturbation phase. This means that the perturbation phase is

Address correspondence and reprint requests to: T. Karino, Utsunomiya University, Utsunomiya, Tochigi 321-8585, Japan. E-mail: dt167105@cc.utsunomiya-u.ac.jp

known, and so the perturbations successively imposed are superposed in the plasma. The HIBs accelerate the fusion target fuel with a large acceleration in inertial fusion. The wobbling HIBs would provide a small oscillating acceleration perturbation in an inertial fusion fuel target during the target implosion. So the RTI growth would be reduced by the phase-controlled superposition of perturbations in heavy-ion inertial fusion (HIF) (Kawata *et al.*, 1993, 2009; Kawata, 2012). In this paper, we discuss the robustness of the dynamic mitigation mechanism for instabilities presented in (Kawata *et al.*, 1993, 2009; Kawata, 2012) and the mitigation of the implosion non-uniformity for the directly driven inertial fusion target by the wobbling HIBs. The results presented here show that the mechanism of the dynamic instability mitigation is viable and rather robust against changes in the phase, amplitude, and wavelength of the wobbling perturbation applied.

2. DYNAMIC INSTABILITY MITIGATION

Let us consider an unstable system, which has one mode of $a = a_0 e^{ikx+\gamma t}$. Here a_0 is the amplitude, $k = 2\pi/\lambda$ is the wave number, λ is the wave length, and γ is the growth rate of the instability. An example initial perturbation is shown in Figure 1a. At $t = 0$, the perturbation is imposed. The initial perturbation grows with γ. After Δt, if another perturbation, which has an inverse phase, is actively imposed (see Fig. 1b), the overall amplitude is the superposition of all the perturbations, and so the actual perturbation amplitude is well mitigated as shown in Figure 1c. This is an ideal example for the dynamic instability mitigation (Kawata *et al.*, 1993, 2009; Kawata, 2012).

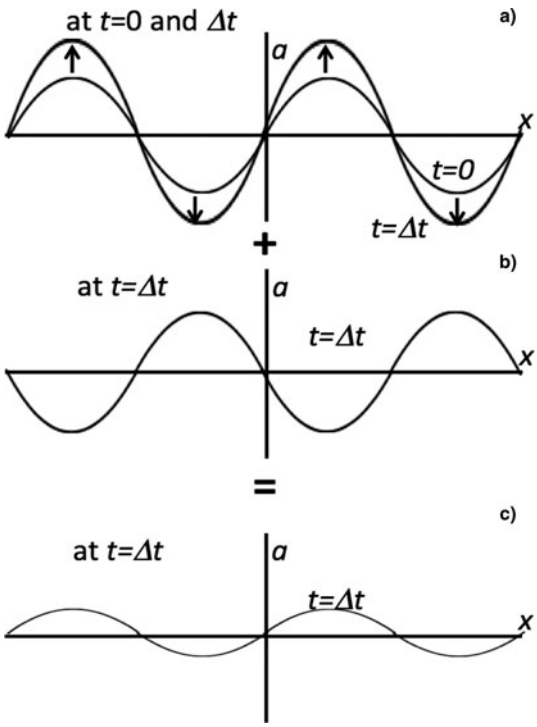

Fig. 1. An ideal example concept of the dynamic mitigation. (a) At $t = 0$ a perturbation is imposed. The initial perturbation grows with γ. (b) After Δt another perturbation, which has an inverse phase, is actively imposed, so that (c) the actual perturbation amplitude is mitigated very well after the superposition of the initial and additional perturbations.

In plasmas the perturbation phase and amplitude cannot be measured. So the perfect feedback control cannot be realized in plasmas and fluids. However, an electron beam can provide its axis wobbling motion or a time-dependent modulation of the beam velocity. A HIB accelerator can also provide a controlled wobbling or oscillating beam with a high frequency (Moretti, 1982; Kawata *et al.*, 2013). They would provide the defined phase and amplitude of perturbations.

When the instability driver wobbles uniformly in time, the imposed perturbation for a physical quantity of F at $t = \tau$ may be written as

$$F = \delta F e^{i\Omega\tau} e^{\gamma(t-\tau)+i\vec{k}\cdot\vec{x}}. \tag{1}$$

Here δF is the amplitude, Ω is the wobbling or oscillation frequency defined actively by the driving wobbler, and $\Omega\tau$ is the phase shift of superimposed perturbations. At each time t, the wobbler or the modulated driver provides a new perturbation with the phase and the amplitude actively defined by the driving wobbler itself. The superposition of the perturbations provides the actual perturbation at t as follows:

$$\int_0^t d\tau \;\; \delta F e^{i\Omega\tau} e^{\gamma(t-\tau)+i\vec{k}\cdot\vec{x}} \propto \frac{\gamma + i\Omega}{\gamma^2 + \Omega^2} \delta F e^{\gamma t} e^{i\vec{k}\cdot\vec{x}} \tag{2}$$

when $\Omega \gg \gamma$, the perturbation amplitude is reduced by the factor of γ/Ω, compared with the pure instability growth ($\Omega = 0$) based on the energy deposition non-uniformity (Kawata *et al.*, 1993, 2009). When $\Omega \cong \gamma$, the amplitude mitigation factor is still about 50%. The result in Eq. (2) presents that the perturbation phase should oscillate with $\Omega \gtrsim \gamma$ for the effective amplitude reduction.

Figure 2 shows an example simulation for RTI, which has a single mode. In this example, two stratified fluids are superimposed under an acceleration of $= g_0 + \delta g$. The density jump ratio between the two fluids is 10/3. In this specific case, the wobbling frequency Ω is γ, the amplitude of δg is $0.1 g_0$, and the results shown in Figure 2 are those at $t = 5/\gamma$. In Figure 2a, δg is constant and drives the RTI as usual, and in Figure 2b, the phase of δg is shifted or oscillates with the frequency of Ω as stated above for the dynamic instability mitigation. The RTI growth mitigation ratio is 72.9% as shown in Figure 2. The growth mitigation ratio is defined by $(H_0 - H_{\text{mitigate}})/H_0 \times 100\%$. Here H is defined as shown in Figure 2a, H_0 shows the deviation amplitude of the two-fluid interface in the case in Figure 2a without the oscillation ($\Omega = 0$), and H_{mitigate} presents the deviation for the other cases with the oscillation ($\Omega \neq 0$). The example

https://doi.org/10.1017/S0263034616000690 Published online by Cambridge University Press

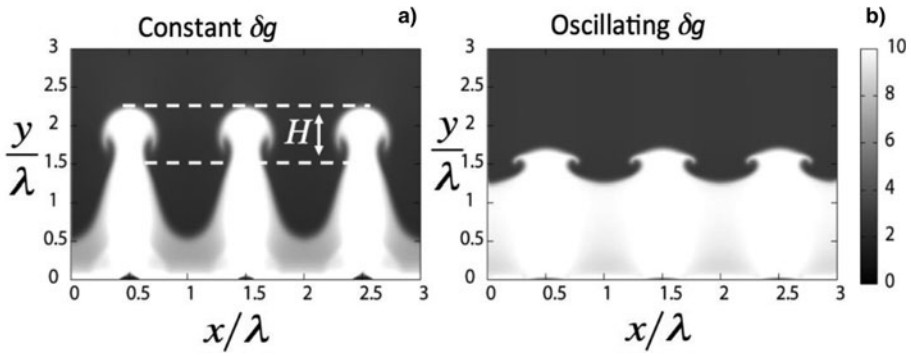

Fig. 2. Example simulation results for the RTI mitigation. δg is 10% of the acceleration g_0 and oscillates with the frequency of $\Omega = \gamma$. As shown above and in Eq. (2), the dynamic instability mitigation mechanism works well to mitigate the instability growth.

simulation results support well the effect of the dynamic mitigation mechanism.

3. ROBUSTNESS OF DYNAMIC MITIGATION OF INSTABILITY

In order to check the robustness of the dynamic instability mitigation mechanism, here we study the effects of the change in the phase, the amplitude and the wavelength of the wobbling perturbation δF, that is, δg in Figure 2 on the dynamic instability mitigation.

When the perturbation amplitude $\delta F = \delta F(t)$ depends on time or oscillates slightly in time, the dynamic mitigation mechanism is examined first. We consider $\delta F(t) = \delta F_0(1 + \Delta e^{i\Omega' t})$ in Eq. (1). Here $\Delta \ll 1$. In this case, Eq. (2) is modified as follows:

$$\int_0^t d\tau\ \delta F e^{i\Omega\tau} e^{\gamma(t-\tau)+i\vec{k}\cdot\vec{x}} \propto \left\{\frac{\gamma + i\Omega}{\gamma^2 + \Omega^2} + \Delta\frac{\gamma + i(\Omega + \Omega')}{\gamma^2 + (\Omega + \Omega')^2}\right\}\delta F_0 e^{\gamma t} e^{i\vec{k}\cdot\vec{x}} \tag{3}$$

when $\Delta \ll 1$ in Eq. (3), just a minor effect appears on the dynamic mitigation of the instability.

We also performed the fluid simulations. In the simulations $\delta F = \delta g(1 - \Delta \sin\Omega' t)$.

The RTI is simulated again based on the same parameter values shown in Figure 2 except the perturbation amplitude oscillation $\delta F(t)$. Figure 3 shows the example simulation results for $\Delta = 0.3$ and $\Omega' = 3\Omega$, Ω, and $\Omega/3$. Figure 3a shows the RTI growth reduction ratio of 72.0% for $\Omega' = \Omega/3$, Figure 3b shows 54.9% for $\Omega' = \Omega$, and Figure 3c shows 72.9% for $\Omega' = 3\Omega$ at $t = 5/\gamma$. The results by the fluid simulations and Eq. (3) demonstrate that the perturbation amplitude oscillation $\delta F = \delta F(t)$ is uninfluential as long as $\Delta \ll 1$.

When the oscillation frequency Ω of the perturbation δF depends on time $[\Omega = \Omega(t)]$, the time-dependent frequency means that $\Omega(t)$ would consist of multiple frequencies: $e^{i\Omega t} = \sum_i \Delta_i e^{i\Omega_i t}$. In this case, Eq. (3) becomes

$$\int_0^t d\tau\ \delta F e^{i\Omega\tau} e^{\gamma(t-\tau)+i\vec{k}\cdot\vec{x}} \propto \sum_i \Delta_i \frac{\gamma + i\Omega_i}{\gamma^2 + \Omega_i^2}\delta F e^{\gamma t} e^{i\vec{k}\cdot\vec{x}}. \tag{4}$$

The result in Eq. (4) shows that the highest frequency of Ω_i contributes to the instability mitigation. In a real system, the highest frequency would be the original wobbling frequency Ω or so, and the largest amplitude of Δ_i is also that for the original wobbling mode. So when the frequency change is slow, the original wobbler frequency of Ω contributes to the mitigation.

The fluid simulations are also done for the RTI with $\Omega(t) = \Omega(1 + \Delta \sin\Omega' t)$ together with the same parameter

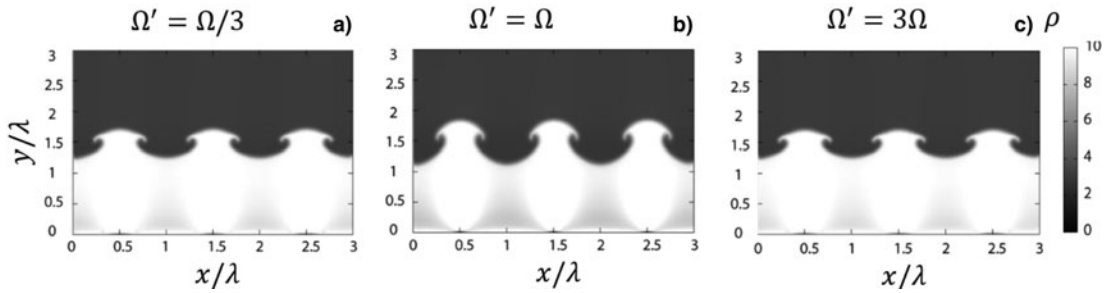

Fig. 3. Fluid simulation results for the RTI mitigation for the time-dependent perturbation amplitude $\delta F = \delta g(1 - \Delta \sin\Omega' t)$ at $t = 5/\gamma$. In the simulations $\Delta = 0.3$, and (a) $\Omega' = \Omega/3$, (b) $\Omega' = \Omega$, and (c) $\Omega' = 3\Omega$. The dynamic mitigation mechanism is also robust against the time change of the perturbation amplitude $\delta F(t)$.

https://doi.org/10.1017/S0263034616000690 Published online by Cambridge University Press

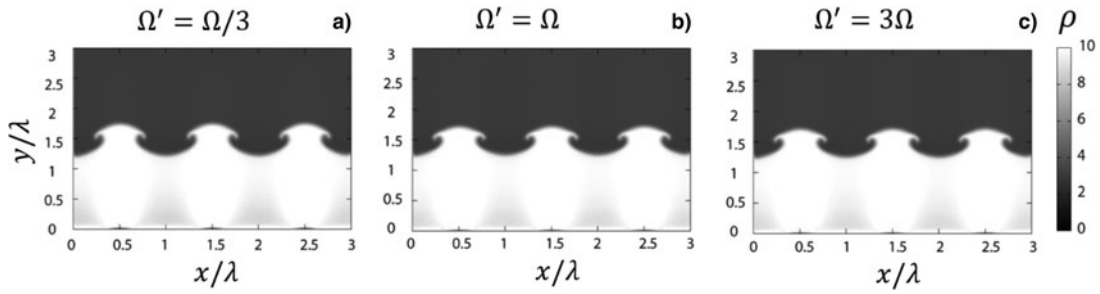

Fig. 4. Fluid simulation results for the RTI mitigation for the time-dependent wobbling frequency $\Omega(t) = \Omega(1 + \Delta\sin\Omega' t)$ at $t = 5/\gamma$. In the simulations $\Delta = 0.3$, and (a) $\Omega' = \Omega/3$, (b) $\Omega' = \Omega$, and (c) $\Omega' = 3\Omega$. The dynamic mitigation mechanism is also robust against the time change of the perturbation frequency $\Omega(t)$.

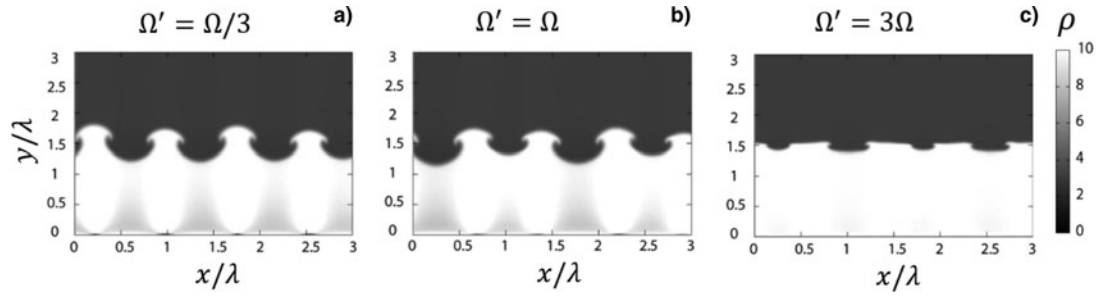

Fig. 5. Fluid simulation results for the RTI mitigation for the time-dependent wobbling wavelength $k(t) = k_0 + \Delta k e^{i\Omega_k' t}$ at $t = 5/\gamma$. In the simulations $\Delta k/k_0 = 0.3$, and (a) $\Omega_k' = \Omega/3$, (b) $\Omega_k' = \Omega$, and (c) $\Omega_k' = 3\Omega$. The dynamic mitigation mechanism is also robust against the time change of the perturbation wavelength $k(t)$.

values employed in Figure 2. Figure 4 shows the example simulation results for $\Delta = 0.3$ and $\Omega' = 3\Omega$, Ω and $\Omega/3$. Figure 4a shows the RTI growth reduction ratio of 66.9% for $\Omega' = \Omega/3$, Figure 4b shows 70.9% for $\Omega' = \Omega$, and Figure 4c shows 72.0% for $\Omega' = 3\Omega$ at $t = 5/\gamma$. The little oscillation of the imposed perturbation oscillation frequency $\Omega(t)$ has a minor effect on the dynamic instability mitigation.

When the wobbling wavelength $\lambda = 2\pi/k$ depends on time, one can expect as follows in a real system: $k(t) = k_0 + \Delta k e^{i\Omega_k' t}$ and $k_0 \gg \Delta k$. In this case, the wobbling wavelength changes slightly in time, and Eq. (3) becomes as follows:

$$\begin{aligned}
&\int_0^t d\tau\ \delta F e^{i\Omega\tau} e^{\gamma(t-\tau)+ik\cdot x} \\
&\propto \delta F e^{\gamma t + ik_0\cdot x} \int_0^t d\tau e^{(i\Omega-\gamma)\tau} \sum_{m=-\infty}^{\infty} i^m J_m(\Delta k\cdot x) e^{im\Omega_k'\tau} \\
&\propto \sum_{m=-\infty}^{\infty} i^m J_m(\Delta k\cdot x) \int_0^t d\tau e^{i(\Omega+m\Omega_k')\tau-\gamma\tau} \\
&\propto \sum_{m=-\infty}^{\infty} i^m J_m(\Delta k\cdot x)\, \frac{\gamma + i\left(\Omega + m\Omega_k'\right)}{\gamma^2 + \left(\Omega + m\Omega_k'\right)^2}.
\end{aligned} \tag{5}$$

Here J_m is the Bessel function of the first kind. The result in Eq. (5) demonstrates that the instability growth reduction effect is not degraded by the small change in the wobbling wavelength. In actual situations the mode $m = 0$ contributes mostly to the instability mitigation, and in this case the original reduction effect shown in Eq. (2) is recovered.

The fluid simulations are also performed for this case $k(t) = k_0 + \Delta k e^{i\Omega_k' t}$. Figure 5 shows the example simulation results for $\Delta k/k_0 = 0.3$ and $\Omega_k' = 3\Omega$, Ω and $\Omega/3$. Figure 5a shows the RTI growth reduction ratio of 61.3% for $\Omega_k' = \Omega/3$, Figure 5b shows 68.0% for $\Omega_k' = \Omega$ and Figure 5c shows 93.3% for $\Omega_k' = 3\Omega$ at $t = 5/\gamma$. For a realistic situation $\Omega_k' \sim \Omega$, where Ω is the wobbling or modulation frequency.

All the results shown above demonstrate that the dynamic instability mitigation mechanism proposed is rather robust against the changes in the amplitude, the phase and the wavelength of the wobbling or modulating perturbation of δF in general or δg in RTI.

4. MITIGATION OF IMPLOSION NON-UNIFORMITY BY SPIRAL WOBBLING HIBS

The oscillating non-uniform acceleration field would be obtained by the HIBs' axes oscillation. We used the heavy ion wobbling beams as the irradiation beams onto a deuterium–tritium (DT) fuel target. Figure 6 shows a schematic diagram for the spiral wobbling beam. For the spiral

https://doi.org/10.1017/S0263034616000690 Published online by Cambridge University Press

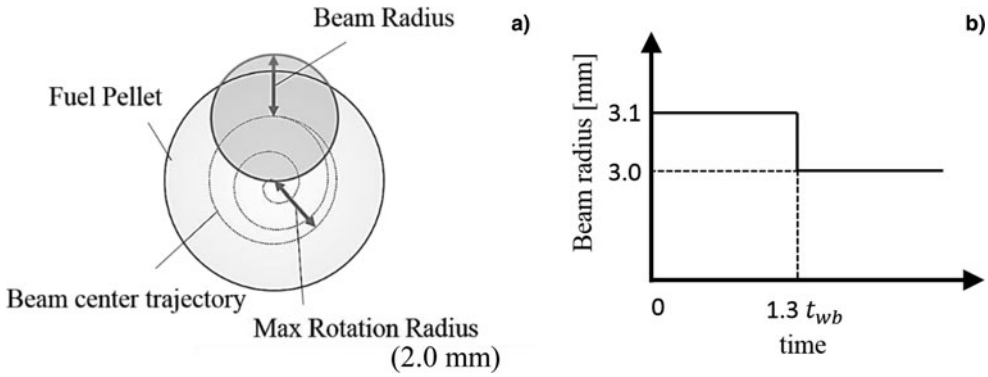

Fig. 6. (a) Schematic diagram for the spiral wobbling beam and (b) Beam radius.

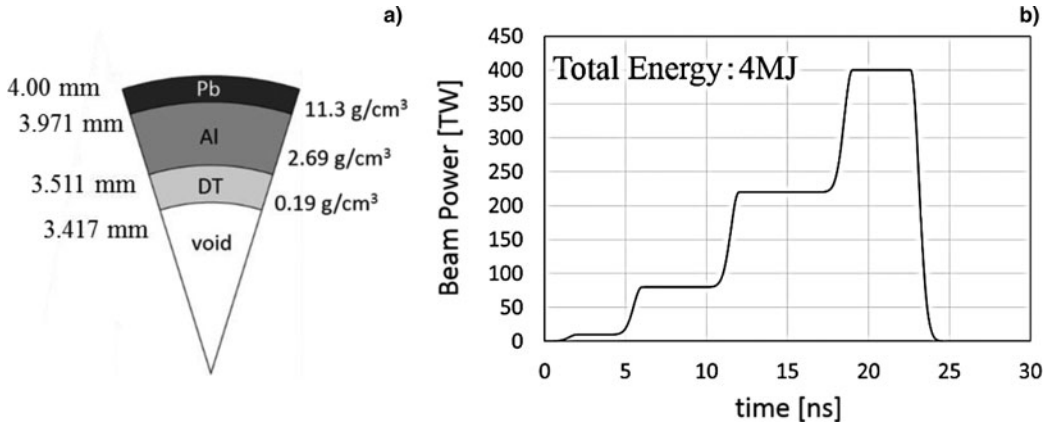

Fig. 7. (a) Target structure and (b) the HIB input pulse.

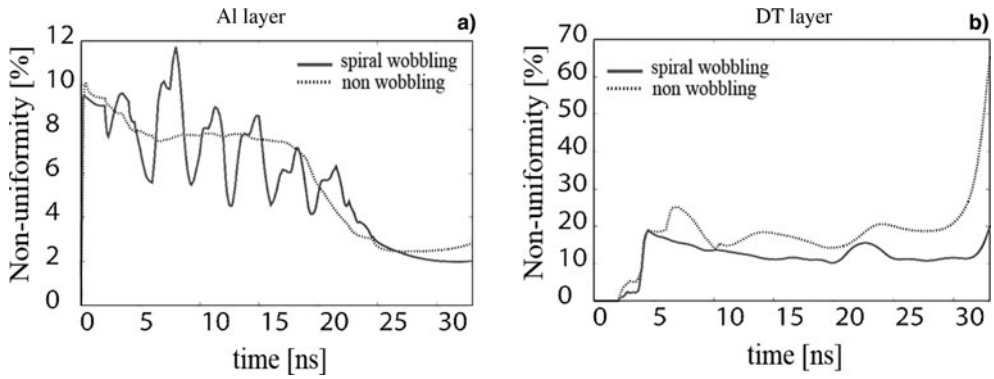

Fig. 8. Non-uniformity histories of the temperature in the Al and DT layers.

wobbling beam, the beam radius changes from 3.1 to 3.0 mm at 1.3 t_{wb} (Fig. 6b). Here $t_{\rm wb}$ is the time for one rotation of the wobbling beam axis. The beam rotation radius becomes 2.0 mm at $t = 2.0\ t_{\rm wb}$ (Kawata *et al.*, 2013) (Fig. 6a). After that, the beam rotation radius is 2.0 mm. When we employ the spiral motion of each HIB axis, the initial imprint of the HIBs illumination non-uniformity is significantly reduced. Figure 7 shows the HIB input pulse and the DT fuel target structure. The Pb beam particle energy is 8 GeV. The total HIB number is 32. The HIB temperature is 100 MeV in the Maxwell distribution.

Figure 8 shows a non-uniformity history of the target temperature, Figure 9 shows a non-uniformity history of the target mass density. The rotation frequency is 200 MHz in this example case. The non-uniformity is evaluated by the total relative root mean square (RMS) as follows:

$$\sigma_{\rm RMS} = \sum_k w_k \sigma_k^{\rm RMS}. \tag{6}$$

https://doi.org/10.1017/S0263034616000690 Published online by Cambridge University Press

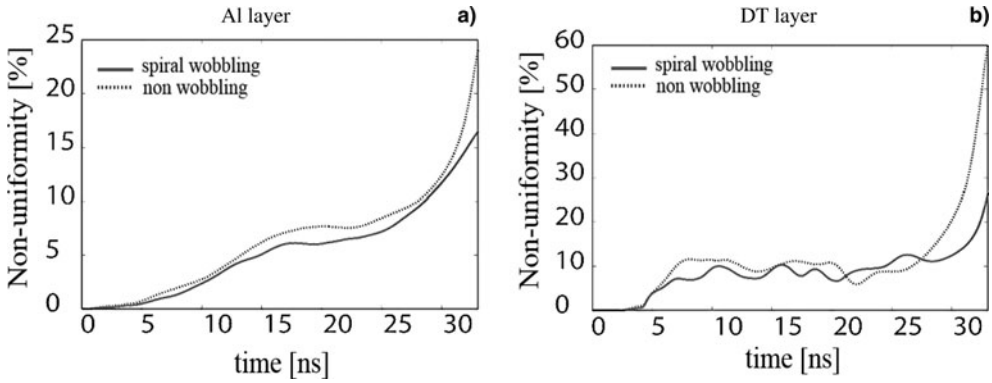

Fig. 9. Non-uniformity histories of the mass density in the Al and DT layers.

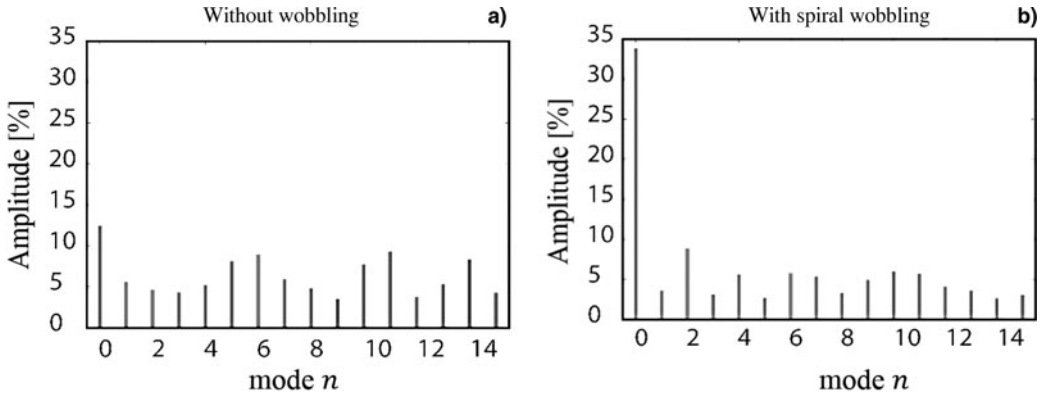

Fig. 10. The mode of the ion temperature in the DT layer ($t = 34$ ns).

Here

$$\sigma_k^{\mathrm{RMS}} = \frac{1}{F_k}\sqrt{\frac{\sum_l (F_{k,l} - F_k)^2}{\theta_{\mathrm{mesh}}}}, \qquad w_k = \frac{\sum_l F_{k,l}}{\sum_k \sum_l F_{k,l}},$$

where F_k is the physical quantity (temperature, density, etc.), F_k is the averaged physical quantity, and w_k is the weight function.

Figures 8 and 9 demonstrate that the implosion non-uniformity of the DT fuel target is reduced with time by the spiral wobbling HIBs. For example, the non-uniformity of the temperature at $t = 34$ ns is relaxed to 19.7% from 72.1% by the wobbling HIBs.

Figure 10 shows the spatial mode of the ion temperature in the DT layer based on the Legendre functions. Figure 10a shows the results without the wobbling motion, and Figure 10b shows the results without the spiral wobbling. It is found that the amplitude of the mode 0 increases significantly by the spiral wobbling HIBs. It means that the implosion symmetry is improved and the implosion non-uniformity was mitigated well.

5. CONCLUSIONS AND DISCUSSIONS

We have discussed the dynamic mitigation method and the mitigation of the implosion non-uniformity for the DT fuel target in HIF. The theoretical and simulation results demonstrate that the dynamic instability mitigation mechanism is viable and rather robust against the changes in the perturbation frequency, the amplitude, and the wavelength of the driver wobbling motion or the driver modulation. We also confirmed the mitigation of the implosion non-uniformity by the spiral wobbling beam by the fluid implosion simulations. It should be mentioned that if the focused beam spot radius becomes smaller for the wobbling beam compared with that for the non-wobbling HIB, the phase space density increases for the HIB particles, and so the additional requirement for the beam quality is imposed (Bangerter *et al*. 2013).

ACKNOWLEDGMENTS

The work was partly supported by JSPS, MEXT, CORE (Center for Optical Research and Education, Utsunomiya University), ILE/Osaka University, and CDI (Creative Department for Innovation, Utsunomiya University). The authors also like to extend their acknowledgements to friends in HIF research group in Japan, in

https://doi.org/10.1017/S0263034616000690 Published online by Cambridge University Press

Tokyo Inst. of Tech., Nagaoka Univ. of Tech., KEK and also in HIF-VNL, USA.

REFERENCES

Atzeni, S. & Meyer-Ter-vehn, J. (2004). *The Physics of Inertial Fusion*. Oxford: Oxford Science Pub.

Bangerter, R.O., Faltens, A. & Seidl, P.A. (2013). Accelerators for Inertial Fusion Energy Prodction. *Reviews of Accelerator Science and Technology* **6**, 85–116.

Betti, R., Mccrory, R.L. & Verdon, C.P. (1993). Stability analysis of unsteady ablation fronts. *Phys. Rev. Lett.* **71**, 3131–3134.

Boris, J.P. (1977). Dynamic stabilization of the imploding shell Rayleigh–Taylor instability. *Comments Plasma Phys. Control. Fusion* **3**, 1–13.

Emery, M.H., Orens, J.H., Gardner, J.H. & Boris, J.P. (1982). Influence of nonuniform laser intensities on ablatively accelerated targets. *Phys. Rev. Lett.* **48**, 253–256.

Kawata, S. (2012). Dynamic mitigation of instabilities. *Phys. Plasmas* **19**, 024503, 1–3.

Kawata, S., Iizuka, Y., Kodera, Y., Ogoyski, A.I. & Kikuchi, T. (2009). Robust fuel target in heavy ion inertial fusion. *Nucl. Instrum. Methods A* **606**, 152–156.

Kawata, S., Kurosaki, T., Koseki, S., Noguchi, K., Barada, D., Ogoyski, A.I., Barnard, J.J. & Logan, B.G. (2013). Wobbling heavy ion beam illumination in heavy ion inertial fusion. *Plasma Fusion Res. Regul. Articles* **8**, 3404048, 1–4.

Kawata, S. & Niu, K. (1984). Effect of nonuniform implosion of target on fusion parameters. *J. Phys. Soc. Jpn.* **53**, 3416–3426.

Kawata, S., Sato, T., Teramoto, T., Bandoh, E., Masubichi, Y., Watanabe, H. & Takahashi, I. (1993). Radiation effect on pellet implosion and Rayleigh–Taylor instability in light-ion beam inertial confinement fusion. *Laser Part. Beams* **11**, 757–768.

Moretti, A. (1982). Utilization of high energy, small emittance accelerators for ICF target experiments. *Nucl. Instrum. Methods* **199**, 557–561.

Nuckolls, J., Wood, L., Thiessen, A. & Zimmmerman, G. (1972). Laser compression of matter to super-high densities: thermonuclear (CTR) applications. *Nature* **239**, 139–142.

Piriz, A.R., Piriz, S.A. & Tahir, N.A. (2011). Dynamic stabilization of classical Rayleigh–Taylor instability. *Phys. Plasmas* **18**, 092705, 1–9.

Piriz, A.R., Prieto, G.R., Diaz, I.M. & Cela, J.J.L. (2010). Dynamic stabilization of Rayleigh–Taylor instability in Newtonian fluids. *Phys. Rev. E* **82**, 026317, 1–11.

Troyon, F. & Gruber, R. (1971). Theory of the dynamic stabilization of the Rayleigh–Taylor instability. *Phys. Fluids* **14**, 2069–2073.

Wolf, G.H. (1970). Dynamic stabilization of the interchange instability of a liquid-gas interface. *Phys. Rev. Lett.* **24**, 444–446.

https://doi.org/10.1017/S0263034616000690 Published online by Cambridge University Press